

RESEARCH ARTICLE

Genetic deletion of *gpr27* alters acylcarnitine metabolism, insulin sensitivity, and glucose homeostasis in zebrafish

Anjali K. Nath^{1,2} | Junyan Ma^{3,4} | Zsu-Zsu Chen¹ | Zhuyun Li³ |
 Maria del Carmen Vitery³ | Michelle L. Kelley³ | Randall T. Peterson⁵ |
 Robert E. Gerszten^{1,2} | Jing-Ruey J. Yeh^{3,4}

¹Division of Cardiovascular Medicine, Beth Israel Deaconess Medical Center, Boston, MA, USA

²Broad Institute, Cambridge, MA, USA

³Cardiovascular Research Center, Massachusetts General Hospital, Charlestown, MA, USA

⁴Department of Medicine, Harvard Medical School, Boston, MA, USA

⁵College of Pharmacy, University of Utah, Salt Lake City, UT, USA

Correspondence

Anjali K. Nath, Division of Cardiovascular Medicine, Beth Israel Deaconess Medical Center, 3 Blackfan Circle, CLS-917, Boston, MA 02215, USA.
 Email: anath1@bidmc.harvard.edu

Jing-Ruey J. Yeh, Cardiovascular Research Center, Massachusetts General Hospital, 149 13th Street, Charlestown, MA, 02129, USA.
 Email: jyeh1@mgh.harvard.edu

Funding information

NIH, Grant/Award Number: U01 MH105027, NIH R21 HG010392 and NIH R01 HL132320-01

Abstract

G protein-coupled receptors (GPCRs) comprise the largest group of membrane receptors in eukaryotic genomes and collectively they regulate nearly all cellular processes. Despite the widely recognized importance of this class of proteins, many GPCRs remain understudied. G protein-coupled receptor 27 (*Gpr27*) is an orphan GPCR that displays high conservation during vertebrate evolution. Although, *GPR27* is known to be expressed in tissues that regulate metabolism including the pancreas, skeletal muscle, and adipose tissue, its functions are poorly characterized. Therefore, to investigate the potential roles of *Gpr27* in energy metabolism, we generated a whole body *gpr27* knockout zebrafish line. Loss of *gpr27* potentiated the elevation in glucose levels induced by pharmacological or nutritional perturbations. We next leveraged a mass spectrometry metabolite profiling platform to identify other potential metabolic functions of *Gpr27*. Notably, genetic deletion of *gpr27* elevated medium-chain acylcarnitines, in particular C6-hexanoylcarnitine, C8-octanoylcarnitine, C9-nonanoylcarnitine, and C10-decanoylcarnitine, lipid species known to be associated with insulin resistance in humans. Concordantly, *gpr27* deletion in zebrafish abrogated insulin-dependent Akt phosphorylation and glucose utilization. Finally, loss of *gpr27* increased the expression of key enzymes in carnitine shuttle complex, in particular the homolog to the brain-specific isoform of *CPT1C* which functions as a hypothalamic energy sensor. In summary, our findings shed light on the biochemical functions of *Gpr27* by illuminating its role in lipid metabolism, insulin signaling, and glucose homeostasis.

KEYWORDS

carnitine palmitoyltransferase I, G protein-coupled receptors, insulin resistance, lipid metabolism, metabolomic profiling

Abbreviations: C2, acetylcarnitine; C3, propionylcarnitine; C3DC, malonylcarnitine; C4, butyrylcarnitine; C4DC, methylmalonylcarnitine; C5, valerylcarnitine; C5DC, glutarylcarnitine; C6, hexanoylcarnitine; C7, heptanoylcarnitine; C8, octanoylcarnitine; C9, nonanoylcarnitine; C10, decanoylcarnitine; C12, dodecanoylcarnitine; C14, tetradecanoylcarnitine; C16, hexadecanoylcarnitine; C18, octadecanoylcarnitine; C18:1, octadecenoylcarnitine; C18:2, octadecadienoylcarnitine; C26, hexacosanoylcarnitine; d.p.f., days post fertilization; *Gpr27*, G protein-coupled receptor 27; SREB, super conserved receptors expressed in the brain.

This is an open access article under the terms of the Creative Commons Attribution-NonCommercial License, which permits use, distribution and reproduction in any medium, provided the original work is properly cited and is not used for commercial purposes.

© 2019 The Authors. The FASEB Journal published by Wiley Periodicals, Inc. on behalf of Federation of American Societies for Experimental Biology

1 | INTRODUCTION

A diverse range of extracellular ligands activate G protein-coupled receptors (GPCRs) including hormones, neurotransmitters, light, peptides, and lipids. Ligand binding triggers interaction with heterotrimeric G proteins and the subsequent activation of intracellular signaling pathways that modulate an incredible array of physiological and disease processes.¹⁻⁴ Notably, pharmacological modulation of GPCRs has proven to be one of the most successful stories in modern medicine; ~34% of all the FDA-approved drugs target human GPCRs.⁵ Thus, GPCRs are widely recognized as an important class of proteins in human biology. However, of the ~800 GPCRs in the genome, there are ~140 GPCRs for which the endogenous ligands and physiological functions are unknown.² Developing tools in model organisms to characterize these GPCRs may uncover many previously unappreciated functions for orphan GPCRs which may enable the future development of therapeutic agents.⁶

Zebrafish have emerged as a powerful model system to elucidate the function of poorly characterized genes.^{7,8} The advantages of this model system are that each female produces hundreds of offspring weekly and that the larvae develop all major organ systems in ~5 d. Moreover, due to their genetic and physiological similarities to humans, zebrafish are a well-established vertebrate organism to study human diseases.⁹⁻¹³ Compared to humans, there is a high degree of conservation in metabolically relevant tissues and biochemical pathways that regulate the endocrine system, skeletal muscle biology, insulin regulation, lipid metabolism, and glucose homeostasis.¹⁴⁻¹⁹ Here, we use this model system to investigate *Gpr27*, an orphan GPCR that belongs to the Super Conserved Receptors Expressed in the Brain (SREB) family of GPCRs and displays very high conservation among vertebrates.²⁰⁻²³

Human gene expression data from the Genotype-Tissue Expression (GTEx) project demonstrated high expression of *GPR27* in the brain. There is also low level expression in several other tissues including the cardiovascular system, pancreas, adrenal glands, skeletal muscle, and adipose tissue, suggesting peripheral functions as well.²⁴ Using an siRNA screen, Ku et al previously showed that, knockdown of *Gpr27* in mouse pancreatic beta cells reduced insulin promoter activity and glucose-stimulated insulin secretion (GSIS),²⁵ implicating its role in cellular energy metabolism. However, to date, studies using whole organism models of loss-of-function *Gpr27* have not been reported. Given that *GPR27* is expressed in several tissues relevant to metabolism, we hypothesized that genetic deletion of *Gpr27* in a whole organism would lead to defects in glucose homeostasis. Furthermore, the application of metabolite profiling approaches to model systems has the potential to reveal novel insights into the effects of genetic perturbations on organismal metabolism and may identify additional metabolic pathways regulated by *Gpr27*.

The growing appreciation for the relationship between circulating metabolites and human health has shed light on the pathogenesis of type 2 diabetes. For example, the development of insulin resistance and diabetes in humans has been associated with the accumulation of medium- and long-chain acylcarnitines in the plasma which is indicative of incomplete fatty acid oxidation.²⁶⁻²⁹ Several lines of evidence in cell and animal models have shown that medium- and long-chain acylcarnitines act as lipid signaling molecules that diminish skeletal muscle response to insulin, thereby providing a potential link between acylcarnitine accumulation and the development of insulin resistance.³⁰⁻³³ However, this phenomenon is not well understood at the molecular level. In particular, the upstream molecular mechanisms that drive acylcarnitine accumulation have yet to be fully elucidated.

In the present work, we generated a zebrafish *gpr27* knockout line and subjected it to energy homeostasis assays to determine the impact of *gpr27* deletion on glucose homeostasis and insulin sensitivity. Further, to identify the potential metabolic actions of *gpr27*, we leveraged a mass spectrometry platform and evaluated a total of 150 polar metabolites. Cumulatively, this study identifies a novel role for *Gpr27* in acylcarnitine metabolism and proposes a potential mechanism by which *Gpr27* regulates glucose homeostasis. In addition, our zebrafish line provides a new *in vivo* tool to study the molecular underpinnings leading to altered acylcarnitine metabolism and defects in insulin-mediated energy homeostasis.

2 | MATERIALS AND METHODS

2.1 | Zebrafish

Animals were maintained and embryos were obtained according to standard fish husbandry protocols. Zebrafish embryos were grown at 28°C in HEPES-buffered Tübingen E3 medium inside light/dark cycle incubators. *gpr27* knockout zebrafish were generated by CRISPR-Cas9 mediated genome editing. The zebrafish *gpr27* gene (ENSDARG0000006607) contains a single exon. The sequence of the target site used to generate the gRNA is GGCATAATTCTGGAGCGAGGGG (the PAM nucleotides are underlined). At the 1-cell stage ~100 ng/μL of sgRNA and 150 ng/μL of Cas9 mRNA were co-injected into the embryo using a glass microcapillary pipette attached to a micromanipulator under a stereomicroscope. The *gpr27* mutant line generated has a 19-bp deletion at position + 39. Genome edits were confirmed by Sanger Sequencing. Founders were outcrossed to establish the F1 generation. F2 generation fish were genotyped using the following PCR primers: 5'-GGGACCAGGACTGCTTAATG-3' (forward) and 5'-AGCCTTGTGGAGTGAGCTGT-3' (reverse).

The PCR products were run on a 2.5% agarose gel. The wild types exhibit a 226 base pair product whereas the knockouts exhibit a 207 base pair band. All methods were carried out in accordance with the regulations and guidelines of the Animal Welfare Act and the American Association for Accreditation of Laboratory Animal Care. All experimental protocols were approved by the IACUC committee at MGH and BIDMC.

2.2 | RT-qPCR

Zebrafish embryos were maintained at 28°C until the desired developmental stages. Subsequently, mRNAs were extracted by TRIzol (Invitrogen) following manufacturer's instruction and further purified using RNA Clean & Concentrator-5 (Zymo Research). cDNAs were synthesized using the QuantiTect Reverse Transcription kit (Qiagen). The quantitative PCR was performed using iTaq Universal SYBR Green Supermix (Bio-Rad). The following PCR primers were used: zEF1a-F, CTGGAGGCCAGCTCAAACAT; zEF1a-R, ATCAAGAAGAGTAGTACCGCTAGCATTAC; zINS-F, TCCACCACCATATCCACCATTTC; zINS-R, CACTGGA CACGACCAACAGG; zGPR27-F, CGCCAAAACAAGAA CGCAGA; zGPR27-R, GGCCGAAAACAACCCAAGAC; zPCK1-F, TGGAGGAGGAGTCAGTCAGC; zPCK1-R, CATGCTGAAGGGGATCACGTA; zGLU2-F, TGCTACT GCTGGTGTGTCCA; zGLUT2-R, CTGCCTTCATTTTCG GCAATGTC; zCPT1A-F, GCTCTTCGGCAAGTCTATCTC; zCPT1A-R, AACACCAGCACGAACCC; zCPT1B-F, TCATGGGCTGACTCTCCTATC; zCPT1B-R, CAATGT CCCTCTGCTGTGTATC; zCPT1C-F, TGTCTTACCAAG CCCTCAATC; zCPT1C-R, CTAGCTGGATAAGCAC CCTTAAT; zCPT2-F, TCTAAATACCACGGGCAACTC; zCPT2-R, GTGCCATTCCTTTTCGAATTAGC; zCRAT-F, GCTATTCAGCTTGCCCTACTACA; zCRAT-R, CGAATG TAGTCTGTTCGTCCTC; zCRATA-F, GAACTCCTCCTT ACAGACCAAC; zCRATA-R, GCTCTCACGGACTCCT TATTG; zACSL1-F, GCTGCCATCACCACATACT; zACSL1-R, GGATAGAGCGACGTGCATATT; zSLC25A 20-F, GACGGCTCCAGAAGGTAAT; zSLC25A20-R, GGCGTTGAAGCCCTTATAGA. The expression of elongation factor 1 alpha (zEF1a) was used for normalization.

2.3 | Glucose measurement

Metformin and glyburide were purchased from Sigma-Aldrich. Larval zebrafish were treated for 24 hours and subsequently glucose was measured. The assay was carried out on larval zebrafish loaded in 96-well plates containing HEPES-buffered Tübingen E3 medium (n = 1 per well). Following exposure to treatments, larvae were frozen at -80°C. Larvae were homogenized in a volume of 50 µL using a motorized

pestle and centrifuged. Glucose levels in the lysates were measured using a glucose oxidase assay³⁴ from Invitrogen (Amplex Red Glucose Assay Kit). Data is represented as the glucose levels per larva.

2.4 | Insulin injections

At 4 days post fertilization (d.p.f.) zebrafish larvae were briefly exposed to tricaine and then placed onto an agarose gel. Pulled glass capillary needles were loaded with vehicle or 10 µg/mL insulin and 1 nL was injected into the circulation.³⁵ The animals were then placed into HEPES-buffered Tübingen E3 medium and returned to the incubator. These studies were conducted in 4 d.p.f. larvae because it has been previously shown that larvae are sensitive to intravascularly administered insulin at this timepoint.³⁵ Further, at later stages as the embryonic tissues thicken, microneedle tip clogging becomes an issue which causes variation in the amount of insulin delivered between animals.

2.5 | Standard and high fat diets

By 7 d.p.f. the nutrients in the yolk sac have been consumed, therefore this timepoint was chosen for feeding experiments.³⁶ A well-established and widely used high fat diet for zebrafish is chicken egg yolks.³⁷ Zebrafish larvae were fed a solution of egg whites (standard diet) or a solution of egg yolks (high fat diet) for 24 hours, as previously described.³⁸

2.6 | Western blots

Zebrafish were lysed in RIPA buffer supplemented with protease and phosphatase inhibitors using a motorized homogenizer. Lysates were run on Bis-Tris gels (4%-20%) in MOPS buffer and transferred to PVDF membranes. Antibodies for AKT and pAKT ser473 were purchased from Cell Signaling (2920S and 4060S).

2.7 | Mass spectrometry

Our platform uses targeted, multiple reaction monitoring MS data acquisition to measure approximately 150 water soluble metabolites that fall into 8 classes: (i) amines; (ii) amino acids and amino acid conjugates; (iii) bile acids; (iv) sugars and sugar phosphates; (v) indoles and indole derivatives; (vi) organic acids; (vii) purines and pyrimidines; (viii) lipids.³⁹ Briefly, metabolites that ionize in the positive ion mode were extracted using acetonitrile and methanol (10 larvae per sample, 10-15 biological replicates per

experimental condition). We used 6 d.p.f. larvae as de-yolkling the embryos to mitigate the effect of highly abundant metabolites suppressing the ionization of other less abundant metabolites is not required. The extracts were separated using hydrophilic interaction liquid chromatography (HILIC) on a 1260 HPLC binary system (Agilent) and the MS analyses were performed in positive ion mode on the QTrap 4000 (Applied Biosystems/Sciex). The coefficients of variation (CV) for analyte measurements generally $\leq 15\%$, and closer to 6% for abundant analytes such as amino acids. Metabolites with CVs $\geq 30\%$ are excluded from analysis. The metabolite data are displayed as the relative delta $[(\text{KO} - \text{WT})/\text{WT}] * 100$. We corrected for multiple comparisons by using a Bonferroni adjusted P value ($P \leq .05/150 = .00033$).

2.8 | Statistics

The data are represented as the mean \pm the standard deviation. Significance was determined using a Student's t test.

3 | RESULTS

3.1 | Generation of the *gpr27* knockout line in zebrafish

The zebrafish *gpr27* gene contains a single exon that produces a 371 amino acid protein (Figure 1A). To determine if developing zebrafish embryos express *gpr27*, real-time quantitative PCR was used. Steadily increasing expression of *gpr27* mRNA was detected in whole zebrafish embryos from 1 to 3 d.p.f.; an 8.5 ± 2.5 fold increase in *gpr27* mRNA was observed in 3 d.p.f. embryos compared to 1 d.p.f. embryos (Figure 1B). To target *gpr27*, we used CRISPR-Cas9 mediated genome editing and confirmed genome edits by Sanger sequencing (Figure S1). One mutant exhibited a 19-nucleotide deletion starting at position + 39, which is expected to cause a frame shift, the generation of a premature stop codon, and the formation of a truncated 41-amino acid protein (Figure 1A and S1). The founder was raised to adulthood and outcrossed to wildtype fish. PCR-based genotyping yielded a 226 base pair product for wildtype *gpr27* and a 207 base pair

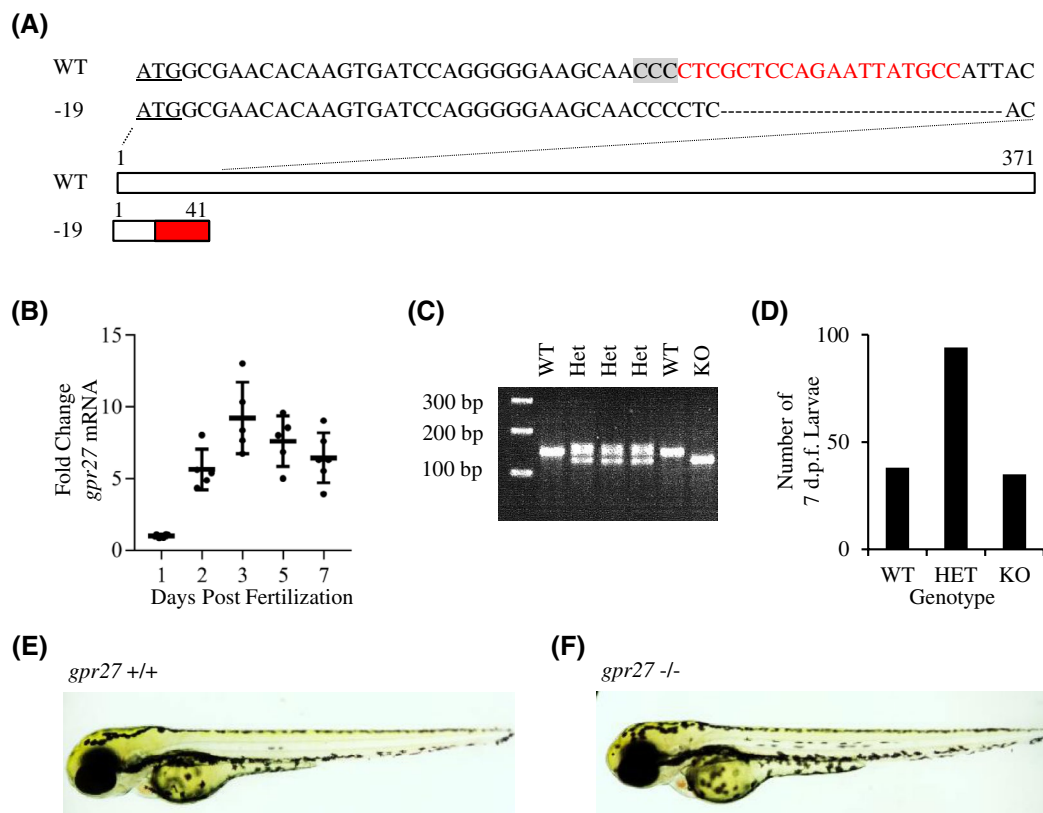


FIGURE 1 Generation of the *gpr27* knockout zebrafish. A, The zebrafish *gpr27* gene contains one exon. The start codon is underlined. The reverse complement of the CRISPR target sequence is marked in red. The protospacer adjacent motif (PAM) of the target site is highlighted by a gray box. A mutant line with a 19-bp deletion (denoted by dashes) was identified. The predicted protein truncation begins at residue 15 (red box). B, *gpr27* mRNA levels in 1-7 d.p.f. embryos ($n = 5-6$ samples of 10 larvae, vertical bars: \pm standard deviation, horizontal bars: mean). C, Image of an agarose gel containing PCR products that represent *gpr27* wildtype and knockout genotypes. D, The number of wildtypes, heterozygotes, and knockouts generated from a heterozygous cross. E-F, Light micrographs of a wildtype and a knockout larva at 5 d.p.f.

product for knockout *gpr27* (Figure 1C). Embryos obtained from heterozygous F1 in-crosses yielded a Mendelian ratio of offspring (Figure 1D, $n = 168$). Further, the knockout embryos displayed normal gross morphology (Figure 1E-F) and the knockout adults lived a normal lifespan.

3.2 | Basal glucose levels and *insulin* gene expression are unaffected in *gpr27* knockout zebrafish

Since a previous study has demonstrated that *Gpr27* regulates insulin promoter activity in MIN6 cells,²⁵ we next assessed *insulin* expression in *gpr27* knockout animals. We measured *insulin* (*ins*) expression in 6 d.p.f. larvae using RT-qPCR and found that there was not a significant difference in *ins* mRNA levels between wildtype and knockout larvae (Figure 2A). Additionally, *pdx1*, a transcriptional activator of the *ins* gene, and *glut2*, a glucose transporter involved in

GSIS, were also unaffected in the *gpr27* knockouts (Figure 2A). We then asked if loss of *gpr27* affects basal glucose levels. Using an established assay,³⁴ glucose was measured at 6 d.p.f. in individual larvae derived from heterozygous crosses. We found that basal glucose levels in the wildtype ($n = 21$), heterozygote ($n = 23$), and knockout ($n = 20$) larvae were not significantly different (Figure 2B).

3.3 | Loss of *gpr27* potentiates the effects of pharmacological and nutritional perturbations that increase glucose levels

Although basal glucose levels were normal in *gpr27* knockouts, we hypothesized that pharmacological and nutritional perturbations which elevate glucose levels would reveal an underlying defect in glucose homeostasis. To increase the glucose levels, we administered hydrocortisone, a known gluconeogenic hormone in mammals and zebrafish.^{34,40} As

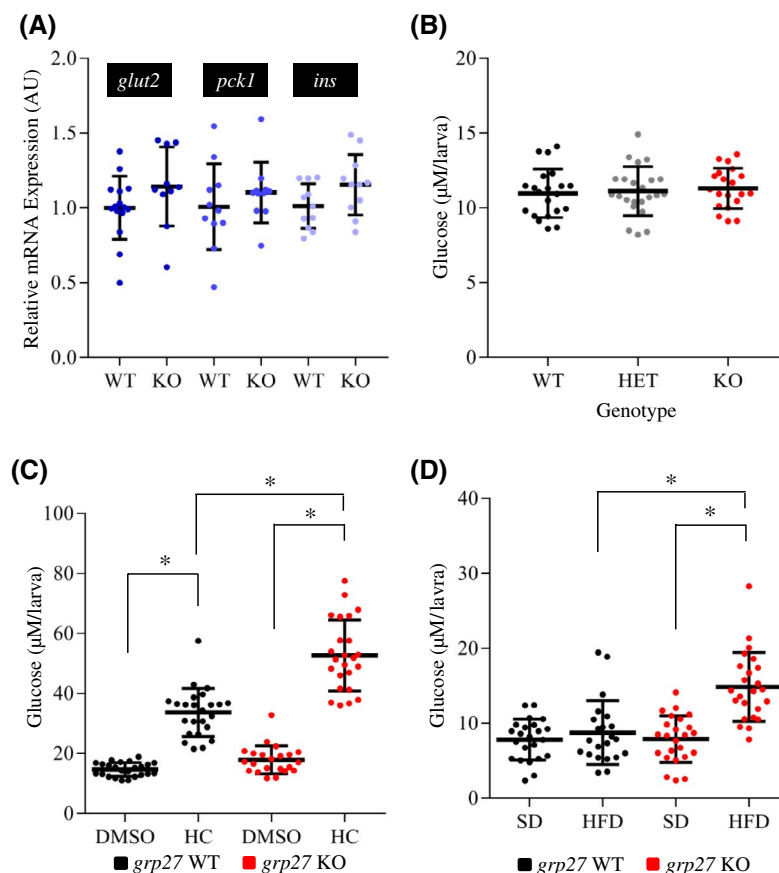


FIGURE 2 Pharmacological and nutritional perturbations that increase glucose levels are exacerbated by loss of *gpr27*. A, Relative expression of *ins*, *pck1*, and *glut2* mRNA in *gpr27* wildtype and knockout larvae ($n = 11$ samples of 10 larvae). B, Glucose levels in 6 d.p.f. larvae generated from heterozygous crosses ($n = 20$ -22 larvae, experiments were replicated at least 3 times). Glucose levels in *gpr27* wildtype and knockout larvae treated with C) DMSO or 100 μM hydrocortisone ($n = 22$ -24 larvae, experiments were replicated at least 3 times). Glucose levels in *gpr27* wildtype and knockout larvae fed a D) standard diet or a high fat diet ($n = 22$ -24 larvae, experiments were replicated at least 3 times). Statistically significant differences between groups are denoted by lines and asterisks ($P < 1\text{E-}07$). Vertical bars denote the standard deviation and horizontal bars denote the mean

expected, the wildtype larvae treated with 100 μM hydrocortisone for 24 hours exhibited significantly increased glucose levels compared to the vehicle treated larvae (33.6 ± 1.6 vs 14.6 ± 2.1 μM , $P = 1\text{E-}11$; Figure 2C). However, *gpr27* knockouts exhibited an even greater response to the gluconeogenic stimulus compared to wildtypes. The *gpr27* KO larvae treated with hydrocortisone displayed an ~57% higher glucose concentration compared to the *gpr27* WT larvae treated with hydrocortisone (52.6 ± 2.3 vs 33.6 ± 1.6 μM , $P = 8\text{E-}8$; Figure 2C).

We next assessed the impact of a short exposure to a high fat diet on glucose homeostasis in *gpr27* knockouts. Zebrafish have been widely used to study lipid metabolism and the effects of elevated dietary fat intake.^{17,37} Further, the regulation of energy homeostasis and the effects of a high fat diet on energy metabolism are conserved between zebrafish and mammals.³⁷ Thus, we fed *gpr27* WT and *gpr27* KO larvae (7 d.p.f.) a standard diet which consisted of mostly proteins or a high fat diet for 24 hours and subsequently measured glucose. The wildtype and knockout larvae that were fed a standard diet exhibited similar glucose levels (7.5 ± 1.2 vs 8.7 ± 1.7 μM ; Figure 2D). Moreover, the high fat diet-fed wildtype larvae were able to maintain normal glucose levels as compared to the standard diet-fed wildtype larvae (7.9 ± 1.2 vs 7.5 ± 1.2 μM ; Figure 2D). However, when the *gpr27* KO larvae were fed a high fat diet, their glucose levels increased ~87% compared to the wildtype larvae fed a high fat diet (14.8 ± 2.6 vs 7.9 ± 1.2 μM , $P = 3\text{E-}07$; Figure 2D). These data suggest an underlying defect in glucose regulation in *gpr27* knockouts. Collectively, the exacerbated elevation in glucose levels in response to the gluconeogenic stimulus or a high fat diet demonstrates that Gpr27 plays an important role in glucose homeostasis in vivo.

3.4 | *gpr27* deletion in zebrafish results in increased medium-chain acylcarnitines

Glucose dysregulation is often interconnected with alterations in other metabolic pathways. Thus, to further characterize the metabolic phenotypes of *gpr27* knockouts and to identify the potential metabolic functions of Gpr27 in an unbiased manner, we used a mass spectrometry platform that captures 150 polar metabolites including amino acids, biogenic amines, tryptophan derivatives, urea cycle intermediates, nucleotides, methyltransferase substrates, acylcarnitines, n-acetyl-l-amino acids, and other polar metabolites (Table S1). Metabolites were extracted from *gpr27* WT and *gpr27* KO larvae at 6 d.p.f. and subjected to metabolite profiling. We used a Bonferroni adjusted P value to correct for multiple comparisons ($P \leq .0003$) and found 13 metabolites that were significantly different in *gpr27* knockouts (Figure

3A). Loss of *gpr27* led to a significant decrease in several amino acids including histidine, glutamine, lysine, asparagine, aspartate, and glycine, as well as in n-acetyl-glutamine and n-carbonyl-beta-alanine (Figure 3B). In addition, we observed a significant increase in 4 metabolites that are acylcarnitine species (Figure 3B).

Acylcarnitines are formed during the transport of long-chain fatty acids into the mitochondria.^{41,42} Subsequently, beta-oxidation results in the complete catabolism of long-chain fatty acids or, in the case of incomplete catabolism, the export of acylcarnitines of varying carbon chain lengths out of the mitochondria. To generate the acylcarnitine profile, our platform captures a total of 19 acylcarnitines spanning distinct fatty acid species containing short-, medium-, and long-carbon chains (Figure 3C). Interestingly, genetic deletion of *gpr27* resulted in a highly significant and specific elevation in medium-chain acylcarnitines, in particular C6-hexanoylcarnitine ($+40.9 \pm 4.9$; $P = 7\text{E-}05$), C8-octanoylcarnitine ($+89.2 \pm 6.1$; $P = 1\text{E-}05$), C9-nonanoylcarnitine ($+86.5 \pm 9.6$; $P = 5\text{E-}06$), and C10-decanoylcarnitine ($+130.1 \pm 8.2$; $P = 6\text{E-}07$). However, short (C2, C3, C3DC, C4, C2DC, C5, and C5DC) and long chain (C12, C14, C16, C18, C18:1, C18:2, and C26) acylcarnitines remained unchanged or modestly changed (Figure 3C, red denotes Bonferroni significant metabolites). In addition, free L-carnitine levels were unchanged (Table S1). Hence, these data demonstrate that genetic deletion of *gpr27* in zebrafish leads to a specific and significant increase in medium-chain acylcarnitines which brings to light a potential role for *gpr27* in the beta-oxidation of fatty acids.

3.5 | *cpt1* gene expression is increased in *gpr27* knockouts

Beta-oxidation of fatty acids occurs in the mitochondria. To enter the mitochondria, long-chain fatty acids must use the carnitine shuttle complex (Figure 3D).^{41,42} Thus, the expression levels of enzymes in this complex control the rate of beta-oxidation. To determine if Gpr27 effects the expression of enzymes in the carnitine shuttle, we measured the mRNA levels of zebrafish homologs of *carnitine palmitoyltransferase I* (isoforms *CPT1A*, *CPT1B*, and *CPT1C*), *carnitine palmitoyltransferase II* (*CPTII*), *carnitine-acylcarnitine translocase* (*SLC25A20*), *carnitine acetyl-CoA transferase* (*CrAT*) and *long-chain acyl-CoA ligase* (*ACSL1*).

In *gpr27* KO larvae, *cpt1cb* was increased by 1.44 fold ($P = .008$) compared to WT larvae (Figure 3E). In addition, *crata* and *cpt1aa* was increased by 1.15 and 1.33 fold, respectively ($P = .03$ and $P = .05$). These findings demonstrate that loss of *gpr27* affects the expression of key enzymes in carnitine shuttle complex, in particular the homologs to the brain and liver isoforms of *CPT1* (*cpt1cb* and *cpt1aa*). These

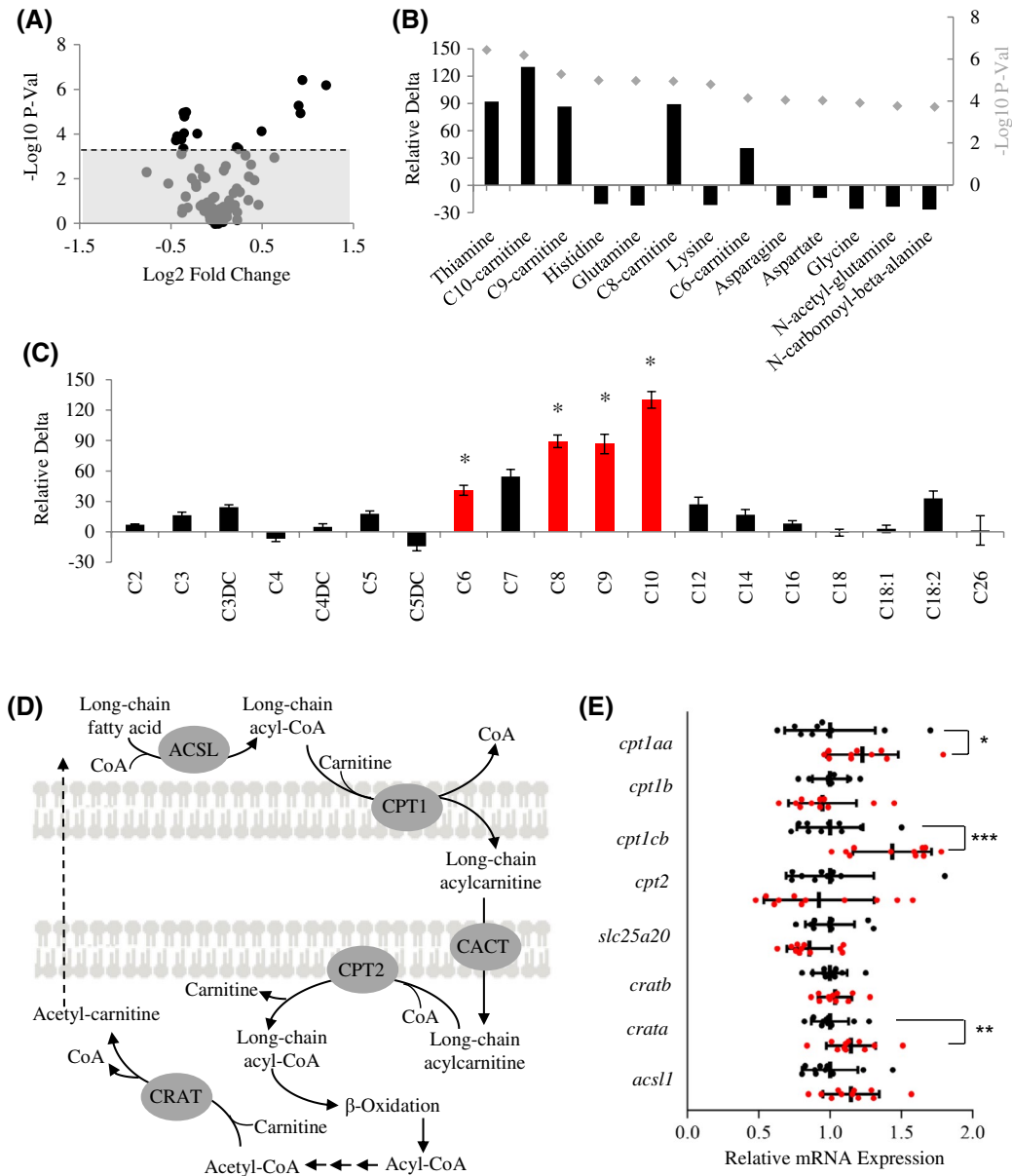


FIGURE 3 Loss of *gpr27* in zebrafish results in increased medium-chain acylcarnitines. A, Volcano plot depicting the P value and fold change of the 150 metabolites measured in *gpr27* knockouts compared to wildtype ($n = 10\text{--}15$ samples of 10 pooled larvae). Metabolites above the gray box reach Bonferroni adjusted significance. B, Relative delta $[(\text{KO} - \text{WT})/\text{WT}] \times 100$ of the 13 Bonferroni significant metabolites identified by mass spectrometry ($P \leq .0003$). The overlaid dot plot depicts the P value. C, Relative delta of the 19 acylcarnitines measured on the platform. Red bars and asterisks denote Bonferroni significant metabolites ($P \leq .0003$). D, Pictorial representation of the carnitine shuttle complex enzymes in the mitochondria. E, Relative expression of *cpt1aa*, *cpt1b*, *cpt1cb*, *cpt2*, *slc25a20*, *cratb*, *crata*, and *acs1l* mRNA in *gpr27* wildtype and knockout larvae ($n = 11$ samples of 10 larvae, vertical bars: \pm SD, horizontal bars: mean, * $P = .05$, ** $P = .03$ and *** $P = .008$)

data also suggest that *Gpr27* may regulate the levels of *Cpt1* thereby altering the levels of acylcarnitine species. Given that acylcarnitines are not merely units of energy but act as lipid signaling molecules, changes in the levels of acylcarnitines might also alter organismal physiology in *gpr27* KO. Further, since the accumulation of medium- and long-chain acylcarnitines has been linked to the development of insulin resistance,^{28,30-32} we hypothesized that loss of *gpr27* affects insulin sensitivity.

3.6 | *gpr27* knockouts are resistant to the glucose lowering effect of exogenous insulin

We next investigated the possibility that *gpr27* deletion contributes to the development of insulin resistance in zebrafish. As in mammalian models, injection of human insulin in the circulation of zebrafish larvae (4 d.p.f.) leads to a decrease in glucose level and an increase in phosphorylated Akt.³⁵ To test if insulin-stimulated glucose utilization is

affected by the loss of *gpr27*, we measured glucose levels in larvae treated with insulin. At 4 d.p.f. vehicle or insulin was injected into the circulation of *gpr27* WT or *gpr27* KO larvae. In wildtype larvae, insulin induced an ~30% reduction in glucose levels (10.6 ± 0.4 vs 15.7 ± 0.5 μM , $P = .0001$; Figure 4A). In contrast, in the *gpr27* knockout larvae, insulin did not significantly affect glucose levels (14.0 ± 0.7 vs 14.3 ± 0.4 μM , Figure 4A). These data demonstrate that *gpr27* knockouts are resistant to the glucose lowering effect of exogenous insulin.

We next performed an orthogonal test using a compound that stimulates insulin secretion. We treated *gpr27* WT and

gpr27 KO larvae with the insulin secretagogue glyburide and measured glucose concentration. As expected, in the wildtype larvae, treatment with 100 nM glyburide induced an ~15% decrease in glucose levels compared to the vehicle-treated larvae ($P = .009$; Figure 4B). In contrast, glyburide did not elicit a significant change in glucose levels in *gpr27* knockouts (Figure 4B), corroborating our findings that *gpr27* mutants are resistant to the glucose lowering effects of insulin administration (Figure 4A). In comparison, we found that both wildtype and knockout larvae responded to metformin, an anti-diabetic drug that primarily reduces glucose levels by inhibiting gluconeogenesis in the

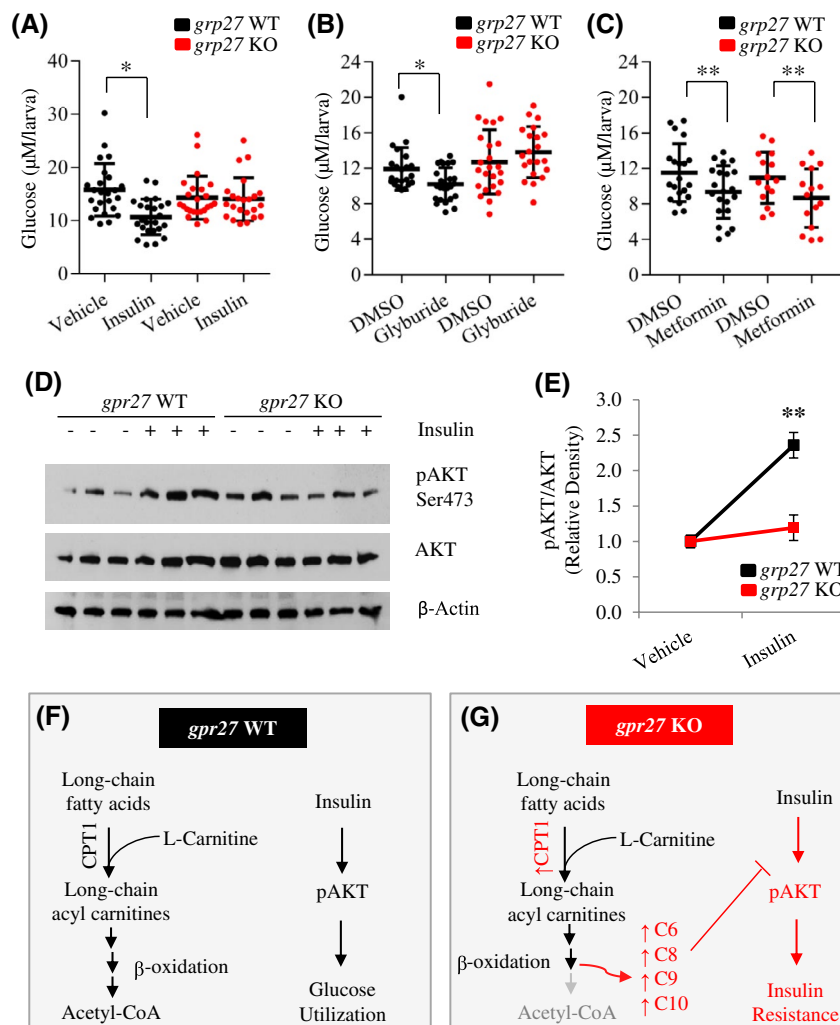


FIGURE 4 Loss of *gpr27* abrogates insulin-mediated Akt phosphorylation and glucose utilization. A, Glucose levels in *gpr27* WT or *gpr27* KO larvae injected with vehicle or insulin ($n = 22-24$ larvae, experiments were replicated at least 3 times). Glucose levels in *gpr27* wildtype and knockout larvae treated with B) DMSO or 100 nM glyburide, or C) DMSO or 100 μM metformin ($n = 22-24$ larvae, experiments were replicated at least 3 times). D, A representative Western blot for pAKT-Ser473 and total Akt in *gpr27* WT or *gpr27* KO larvae injected with vehicle or insulin (3 biological replicates of 10 pooled embryos). E, Quantification of Western blot results (9 biological replicates of 10 pooled embryos). F-G, In wildtype larvae, long-chain fatty acids enter the mitochondria using the carnitine shuttle complex and undergo beta-oxidation to form acetyl-CoA. However, loss of *gpr27* increases the expression of CPT1 enzymes and leads to incomplete beta-oxidation which results in increased medium-chain acylcarnitines, abrogated pAKT levels, and diminished insulin-stimulated glucose utilization. Data are represented as the mean \pm standard deviation. Statistically significant differences between groups are denoted by lines and asterisks (* $P < .009$, ** $P \leq .02$)

liver. Metformin (100 μ M) significantly decreased the level of glucose in wildtype larvae by \sim 19% ($P = .01$) and in knockout larvae by \sim 20% (Figure 4C; $P = .02$). Currently, insulin protein cannot yet be reliably measured in zebrafish,³⁷ therefore we are unable to confirm that glyburide induces similar levels of insulin secretion in wildtypes and knockouts. However, collectively our findings that both insulin injection and glyburide treatment do not lower glucose levels in *gpr27* knockouts imply that loss of *gpr27* diminishes insulin action.

3.7 | Loss of *gpr27* abrogates Akt-dependent insulin signaling

We next sought to determine if there was a defect in insulin signaling in *gpr27* KO zebrafish. Akt signaling plays a central role in insulin-stimulated glucose uptake in peripheral tissues in both mammals and zebrafish^{43,44}; therefore, we examined if insulin-mediated Akt phosphorylation was affected by genetic deletion of *gpr27*. Following a 2-h incubation period, lysates were generated and subjected to Western blotting for p-Akt (Ser473) and total Akt (Figure 4D-E). As expected, administration of insulin to wildtype larvae resulted in a significant 2.35 fold increase in p-Akt levels compared to vehicle-treated larvae ($P = .04$). In contrast, *gpr27* KO larvae showed only a slight increase in Akt phosphorylation in response to insulin treatment. Insulin-treated *gpr27* KO larvae displayed significantly less insulin-induced p-Akt (Ser 473) compared to insulin-treated *gpr27* WT larvae (1.19 fold increase vs 2.35 fold increase, $P = .02$; Figure 4E). Finally, there was not a statistically significant difference in total AKT levels. These data demonstrate that insulin-dependent Akt phosphorylation is abrogated in *gpr27* KO zebrafish and suggest that loss of *gpr27* contributes to insulin insensitivity.

In summary, this study shows that loss of *gpr27* results in diet-induced glucose dysregulation, increased *cpt1* expression and increased medium-chain acylcarnitines, abrogated insulin-mediated Akt phosphorylation, and reduced insulin-stimulated glucose utilization. Taken together, the phenotypes in our whole body *gpr27* knockout line revealed connections between *gpr27*, acylcarnitine metabolism, and lipid-induced insulin resistance (Figure 4F-G).

4 | DISCUSSION

Insulin resistance is a major cause of type 2 diabetes and a risk factor for other debilitating health conditions such as cardiovascular disease, cancer, and obesity.^{45,46} Although it is known that the development of insulin resistance contributes to the etiology of several human diseases, the phenomenon

remains poorly understood at the molecular level.^{47,48} This study identifies *Gpr27* as a previously unknown player in the development of insulin resistance and presents new opportunities for dissecting the molecular pathways leading to defects in insulin action.

By generating and phenotyping the first whole-body *gpr27* knockout line, we found that loss of *gpr27* leads to defects in glucose homeostasis and insulin signaling. Administration of glucose-elevating perturbations, such as a high fat diet or a glucocorticoid, resulted in significantly higher glucose level in *gpr27* KO zebrafish compared to wildtypes. However, in contrast to a previous study that found decreased *insulin* gene expression by siRNA-mediated *Gpr27* knockdown in mouse pancreatic beta cells,²⁵ we did not find a significant difference in the *insulin* mRNA levels between the *gpr27* wildtype and knockout zebrafish. However, *GPR27* is also known to be expressed by several other tissues in addition to the pancreas. Moreover, glucose homeostasis is modulated by intricate intra-tissue communications that cannot be fully replicated in cell-based assays. Our data indicate that insulin sensitivity is diminished in *gpr27* KO animals as evidenced by abrogated Akt phosphorylation and glucose utilization upon insulin treatment. These findings suggest that dysregulation of the GPR27 signaling pathway may have an unappreciated role in the development of insulin resistance in humans.

Insulin resistance in diabetic and nondiabetic individuals has been associated with elevations in free fatty acids such as acylcarnitines.^{26,29,32} Using a metabolite profiling approach, we found that *gpr27* knockouts manifested a specific acylcarnitine accumulation phenotype. Genetic deletion of *gpr27* resulted in elevated medium-chain acylcarnitines, whereas short- and long-chain acylcarnitines were unaffected. Together, these data provide mechanistic insight into the role of *gpr27* in energy homeostasis by suggesting that loss of *gpr27* leads to incomplete fatty acid oxidation. Fatty acid oxidation occurs in the mitochondria and the rate limiting step in beta-oxidation is CPT1.^{41,42} We found that loss of *gpr27* leads to increase expression of the liver isoform of *cpt1* and a highly significant increase in expression of the zebrafish homologue of *CPT1C*. *CPT1C* is predominantly expressed in the brain.⁴⁹ Interestingly, *CPT1C* does not play a role in fatty acid oxidation, rather it acts as a hypothalamic energy sensor.⁵⁰ These findings suggest that *Gpr27* may regulate lipid metabolism by transcriptional regulation of CPT1 enzymes.

Following transport into the mitochondria via CPT1 enzymes, if fatty acids are not completely oxidized to acetyl-CoA, mitochondria-derived incompletely oxidized acylcarnitines are able to cross cell membranes, enter the circulation, and act as lipid signaling molecules. Therefore, the acylcarnitine profile of *gpr27* knockouts raises the possibility that the primary defect in *gpr27* knockout animals

is altered lipid metabolism which subsequently leads to lipid-induced insulin resistance. Our findings are consistent with previous studies that suggest a causative role for acylcarnitines in the genesis of insulin resistance. Mice that were treated for 2 weeks with medium-chain acylcarnitines (C6 and C8) exhibited normal fasting glucose levels.³² However, a glucose challenge revealed an underlying glucose intolerance phenotype.³² Moreover, skeletal muscle cells treated with C4, C14, and C16 acylcarnitines displayed decreased insulin-stimulated glucose uptake and decreased insulin-mediated Akt phosphorylation.³⁰ Our data extend prior studies by implicating a role for GPR27 in fatty acid metabolism, thereby providing new insights into the regulation of acylcarnitines and their impact on insulin sensitivity.

Although a growing body of literature from both animal and human studies has shown that acylcarnitines contribute causally to the development of insulin resistance, prior to the development of overt disease, the upstream molecular mechanisms that precede these defects are largely unknown.^{26,29,32} We speculate that Gpr27 regulates acylcarnitine metabolism and that the subsequent accumulation of acylcarnitines influences insulin-mediated glucose homeostasis (Figure 4F-G). Thus, further investigations in the *gpr27* zebrafish model may enhance our understanding of how an altered lipid profile leads to impaired insulin signaling. For instance, lipid overload has been linked to oxidative stress, reduced mitochondrial respiratory capacity, and inhibition of glucose-coupled insulin secretion.⁵¹ Therefore, future studies to determine if *gpr27* knockouts exhibit mitochondrial dysfunction and to measure mitochondrial capacity in *gpr27* knockouts are warranted. Notably, *gpr27* knockouts exhibit normal basal glucose levels and normal gross morphology suggesting that there is not generalized failure of mitochondrial function in these animals. Moreover, lipid overload may lead to metabolic inflexibility. The metabolic inflexibility theory postulates that an imbalance between glucose and fatty acid oxidation results in defects in fuel switching, such as in the fasting-to-fed transition, which may subsequently cause glucose utilization defects.⁵² Hence, it will be important to determine if loss of *gpr27* affects the rates of fatty acid and glucose oxidation, in addition to fuel selection. Finally, a detailed analysis of the insulin receptor signaling axis may reveal crucial links between the metabolic phenotypes and the insulin signal transduction defects in the *gpr27* knockouts.

Our study does have some limitations. First, we cannot discern the tissue source of accumulated acylcarnitines and insulin resistance. In the future, tissue-specific analyses may shed new light on the cross talk between tissue and systemic phenotypes in these fish. Moreover, it will be useful to generate tissue-specific *gpr27* knockouts in order to determine whether it functions in the brain, muscle, or other

peripheral tissues. Second, we proposed that alterations in fatty acid metabolism rather than glucose metabolism are the primary defect in *gpr27* KO zebrafish based on the following findings: (i) basal glucose levels are normal in the knockouts in spite of elevated acylcarnitines and (ii) exposure to a high fat diet leads to glucose dysregulation. However, we acknowledge that *gpr27* may also affect lipid transport. Therefore, to fully delineate the role of Gpr27 in lipid biology, a comprehensive lipid metabolite analysis following standard and high fat diets will be required in addition to lipid transport studies. Finally, an exciting alternative interpretation of our data is that Gpr27 is a lipid sensor that regulates lipid metabolism. Indeed, many lipid species such as free fatty acids, glycerophospholipids, and sphingolipids are known ligands of GPCRs.^{53,54} Thus, future investigations will be conducted to determine if acylcarnitines or other lipid species are bona fide ligands of Gpr27.

In conclusion, elucidating the functions of orphan GPCRs in a tractable whole organism model such as the zebrafish is a powerful approach that can reveal unappreciated insights into their in vivo biology. Further, applying metabolic analysis to model systems can help guide mechanistic understanding of phenotypes observed in model organisms. In the present study, we coupled glucose assays with metabolomics analysis and discovered a novel role for *gpr27* in acylcarnitine metabolism, insulin sensitivity, and glucose homeostasis in zebrafish. These findings suggest that dysregulated GPR27 signaling may play a role in diabetes or other metabolic syndromes in humans. Finally, this zebrafish line will enable future investigations on the molecular connections between *gpr27*, lipid metabolism, and insulin-mediated energy homeostasis.

ACKNOWLEDGMENTS

This work is dedicated to Maria del Carmen Vitery who passed away on January 16, 2019. Her unyielding passion for science and her hard work helped this project taking shape in its early stages. This work was supported by NIH U01 MH105027 (JY), NIH R21 HG010392 (AKN), and NIH R01 HL132320-01 (REG).

CONFLICT OF INTEREST

The authors have no competing interests.

AUTHOR CONTRIBUTIONS

A.K. Nath, J. Ma, Z.-Z. Chen, Z. Li, M.d.C. Vitery, and M.L. Kelley performed the experiments. A.K. Nath and J.-R.J. Yeh conceived the project and supervised the work. A.K. Nath wrote the original draft of the manuscript. A.K. Nath and J.-R.J. Yeh revised the manuscript. R.E. Gerszten and RT Peterson contributed to the ideas of the project and the final manuscript. A.K. Nath, R.E. Gerszten, R.T. Peterson, and J.-R.J. Yeh provided the resources for the project.

REFERENCES

- Reimann F, Gribble FM. G protein-coupled receptors as new therapeutic targets for type 2 diabetes. *Diabetologia*. 2016;59:229-233.
- Lagerstrom MC, Schioth HB. Structural diversity of G protein-coupled receptors and significance for drug discovery. *Nat Rev Drug Discov*. 2008;7:339-357.
- Hamm HE. The many faces of G protein signaling. *J Biol Chem*. 1998;273:669-672.
- Foster SR, Roura E, Molenaar P, Thomas WG. G protein-coupled receptors in cardiac biology: old and new receptors. *Biophys Rev*. 2015;7:77-89.
- Hauser AS, Attwood MM, Rask-Andersen M, Schioth HB, Gloriam DE. Trends in GPCR drug discovery: new agents, targets and indications. *Nat Rev Drug Discov*. 2017;16:829-842.
- Oprea TI, Bologa CG, Brunak S, et al. Unexplored therapeutic opportunities in the human genome. *Nat Rev Drug Discov*. 2018;17:317-332.
- Kettleborough RN, Busch-Nentwich EM, Harvey SA, et al. A systematic genome-wide analysis of zebrafish protein-coding gene function. *Nature*. 2013;496:494-497.
- Shim H, Kim JH, Kim CY, et al. Function-driven discovery of disease genes in zebrafish using an integrated genomics big data resource. *Nucleic Acids Res*. 2016;44:9611-9623.
- Howe K, Clark MD, Torroja CF, et al. The zebrafish reference genome sequence and its relationship to the human genome. *Nature*. 2013;496:498-503.
- Santoriello C, Zon LI. Hooked! Modeling human disease in zebrafish. *J Clin Invest*. 2012;122:2337-2343.
- Sinner MF, Tucker NR, Lunetta KL, et al. Integrating genetic, transcriptional, and functional analyses to identify 5 novel genes for atrial fibrillation. *Circulation*. 2014;130:1225-1235.
- Liu LY, Fox CS, North TE, Goessling W. Functional validation of GWAS gene candidates for abnormal liver function during zebrafish liver development. *Dis Model Mech*. 2013;6:1271-1278.
- Wagner BK, Gilbert TJ, Hanai J, et al. A small-molecule screening strategy to identify suppressors of statin myopathy. *ACS Chem Biol*. 2011;6:900-904.
- Gut P, Reischauer S, Stainier DYR, Arnaout R. Little fish, big data: zebrafish as a model for cardiovascular and metabolic disease. *Physiol Rev*. 2017;97:889-938.
- Schlegel A, Gut P. Metabolic insights from zebrafish genetics, physiology, and chemical biology. *Cell Mol Life Sci*. 2015;72:2249-2260.
- Huang W, Wang G, Delaspre F, Vitery MdC, Beer RL, Parsons MJ. Retinoic acid plays an evolutionarily conserved and biphasic role in pancreas development. *Dev Biol*. 2014;394:83-93.
- Quinlivan VH, Farber SA. Lipid uptake, metabolism, and transport in the larval zebrafish. *Front Endocrinol (Lausanne)*. 2017;8:319.
- Nevis K, Obregon P, Walsh C, Guner-Ataman B, Burns CG, Burns CE. Tbx1 is required for second heart field proliferation in zebrafish. *Dev Dyn*. 2013;242:550-559.
- Prince VE, Anderson RM, Dalgin G. Zebrafish pancreas development and regeneration: fishing for diabetes therapies. *Curr Top Dev Biol*. 2017;124:235-276.
- Matsumoto M, Saito T, Takasaki J, et al. An evolutionarily conserved G-protein coupled receptor family, SREB, expressed in the central nervous system. *Biochem Biophys Res Commun*. 2000;272:576-582.
- Dupuis N, Laschet C, Franssen D, et al. Activation of the orphan G protein-coupled receptor GPR27 by surrogate ligands promotes beta-arrestin 2 recruitment. *Mol Pharmacol*. 2017;91:595-608.
- Yanai T, Kurosawa A, Nikaido Y, et al. Identification and molecular docking studies for novel inverse agonists of SREB, super conserved receptor expressed in brain. *Genes Cells*. 2016;21:717-727.
- Martin AL, Steurer MA, Aronstam RS. Constitutive activity among orphan class-A G protein coupled receptors. *PLoS One*. 2015;10:e0138463.
- Consortium GT. The genotype-tissue expression (GTEx) project. *Nat Genet*. 2013;45:580-585.
- Ku GM, Pappalardo Z, Luo CC, German MS, McManus MT. An siRNA screen in pancreatic beta cells reveals a role for Gpr27 in insulin production. *PLoS Genet*. 2012;8:e1002449.
- Mai M, Tonjes A, Kovacs P, Stumvoll M, Fiedler GM, Leichtle AB. Serum levels of acylcarnitines are altered in prediabetic conditions. *PLoS One*. 2013;8:e82459.
- Mihalik SJ, Goodpaster BH, Kelley DE, et al. Increased levels of plasma acylcarnitines in obesity and type 2 diabetes and identification of a marker of glucolipotoxicity. *Obesity (Silver Spring)*. 2010;18:1695-1700.
- Nowak C, Hetty S, Salihovic S, et al. Glucose challenge metabolomics implicates medium-chain acylcarnitines in insulin resistance. *Sci Rep*. 2018;8:8691.
- Adams SH, Hoppel CL, Lok KH, et al. Plasma acylcarnitine profiles suggest incomplete long-chain fatty acid beta-oxidation and altered tricarboxylic acid cycle activity in type 2 diabetic African-American women. *J Nutr*. 2009;139:1073-1081.
- Aguer C, McCoin CS, Knotts TA, et al. Acylcarnitines: potential implications for skeletal muscle insulin resistance. *FASEB J*. 2015;29:336-345.
- Wolf M, Chen S, Zhao X, et al. Production and release of acylcarnitines by primary myotubes reflect the differences in fasting fat oxidation of the donors. *J Clin Endocrinol Metab*. 2013;98:E1137-1142.
- Batchuluun B, Al Rijjal D, Prentice KJ, et al. Elevated medium-chain acylcarnitines are associated with gestational diabetes mellitus and early progression to Type 2 diabetes and induce pancreatic beta-cell dysfunction. *Diabetes*. 2018;67:885-897.
- Samuel VT, Petersen KF, Shulman GI. Lipid-induced insulin resistance: unravelling the mechanism. *Lancet*. 2010;375:2267-2277.
- Nath AK, Ryu JH, Jin YN, et al. PTPMT1 inhibition lowers glucose through Succinate dehydrogenase phosphorylation. *Cell Rep*. 2015;10:694-701.
- Marin-Juez R, Jong-Raadsen S, Yang S, Spaink HP. Hyperinsulinemia induces insulin resistance and immune suppression via Ptpn6/Shp1 in zebrafish. *J Endocrinol*. 2014;222:229-241.
- Schlegel A, Stainier DY. Microsomal triglyceride transfer protein is required for yolk lipid utilization and absorption of dietary lipids in zebrafish larvae. *Biochemistry*. 2006;45:15179-15187.
- Zang L, Maddison LA, Chen W. Zebrafish as a model for obesity and diabetes. *Front Cell Dev Biol*. 2018;6:91.
- den Broeder MJ, Moester MJB, Kamstra JH, et al. Altered adipogenesis in zebrafish larvae following high fat diet and chemical exposure is visualised by stimulated raman scattering microscopy. *Int J Mol Sci*. 2017;18.
- Wang TJ, Larson MG, Vasani RS, et al. Metabolite profiles and the risk of developing diabetes. *Nat Med*. 2011;17:448-453.
- Lecocq FR, Mebane D, Madison LL. The acute effect of hydrocortisone on hepatic glucose output and peripheral glucose utilization. *J Clin Invest*. 1964;43:237-246.

41. Schulz H. Beta oxidation of fatty acids. *Biochim Biophys Acta*. 1991;1081:109-120.
42. Indiveri C, Iacobazzi V, Tonazzi A, et al. The mitochondrial carnitine/acylcarnitine carrier: function, structure and physiopathology. *Mol Aspects Med*. 2011;32:223-233.
43. Sharma N, Arias EB, Bhat AD, et al. Mechanisms for increased insulin-stimulated Akt phosphorylation and glucose uptake in fast- and slow-twitch skeletal muscles of calorie-restricted rats. *Am J Physiol Endocrinol Metab*. 2011;300:E966-978.
44. Maddison LA, Joest KE, Kammeyer RM, Chen W. Skeletal muscle insulin resistance in zebrafish induces alterations in beta-cell number and glucose tolerance in an age- and diet-dependent manner. *Am J Physiol Endocrinol Metab*. 2015;308:E662-669.
45. Avgerinos KI, Spyrou N, Mantzoros CS, Dalamaga M. Obesity and cancer risk: emerging biological mechanisms and perspectives. *Metabolism*. 2019;92:121-135.
46. Laakso M, Kuusisto J. Insulin resistance and hyperglycaemia in cardiovascular disease development. *Nat Rev Endocrinol*. 2014;10:293-302.
47. Friesen M, Cowan CA. Adipocyte metabolism and insulin signaling perturbations: insights from genetics. *Trends Endocrinol Metab*. 2019;30:396-406.
48. Yang Q, Vijayakumar A, Kahn BB. Metabolites as regulators of insulin sensitivity and metabolism. *Nat Rev Mol Cell Biol*. 2018;19:654-672.
49. Price N, van der Leij F, Jackson V, et al. A novel brain-expressed protein related to carnitine palmitoyltransferase I. *Genomics*. 2002;80:433-442.
50. Wolfgang MJ, Kurama T, Dai Y, et al. The brain-specific carnitine palmitoyltransferase-1c regulates energy homeostasis. *Proc Natl Acad Sci U S A*. 2006;103:7282-7287.
51. Chow L, From A, Seaquist E. Skeletal muscle insulin resistance: the interplay of local lipid excess and mitochondrial dysfunction. *Metabolism*. 2010;59:70-85.
52. Goodpaster BH, Sparks LM. Metabolic flexibility in health and disease. *Cell Metab*. 2017;25:1027-1036.
53. Costanzi S, Neumann S, Gershengorn MC. Seven transmembrane-spanning receptors for free fatty acids as therapeutic targets for diabetes mellitus: pharmacological, phylogenetic, and drug discovery aspects. *J Biol Chem*. 2008;283:16269-16273.
54. Hanson MA, Roth CB, Jo E, et al. Crystal structure of a lipid G protein-coupled receptor. *Science*. 2012;335:851-855.

SUPPORTING INFORMATION

Additional supporting information may be found online in the Supporting Information section.

How to cite this article: Nath AK, Ma J, Chen Z-Z, et al. Genetic deletion of *gpr27* alters acylcarnitine metabolism, insulin sensitivity, and glucose homeostasis in zebrafish. *The FASEB Journal*. 2020;34:1546–1557. <https://doi.org/10.1096/fj.201901466R>